JMEPEG (2010) 19:1058–1064
DOI: 10.1007/s11665-009-9578-4

1059-9495/$19.00

Impact Energy of Functionally Graded Steels in Crack Arrester Configuration

A. Nazari and J. Aghazadeh Mohandesi

(Submitted March 14, 2009; in revised form September 7, 2009)

Charpy impact energy of functionally graded steels produced by electroslag remelting composed of graded ferrite and austenite layers together with bainite or martensite intermediate layer in the form of crack arrester configuration has been investigated. The results obtained in the present study indicate that the notch tip position with respect to bainite or martensite layer significantly affects the impact energy. The closer the notch tip to the tougher layer, the higher the impact energy of the composite due to increment of energy absorbed by plastic deformation zone ahead of the notch and vice versa. Empirical relationships have been determined to correlate the impact energy of functionally graded steels to the morphology of layers.

Keywords crack arrester, distance of notch, functionally graded steel, impact energy, plastic zone

1. Introduction

Functionally graded materials (FGMs) are multi-phase systems in which composition varies gradually in some directions to obtain unique mechanical, thermal, and electrical properties that distinguish them from the conventional composites which in general are of discrete, piecewise nature with sharp interfaces (Ref 1-4). To date very few fracture experiments involving FGMs, particularly on dynamic fracture, have been reported. Over the last 50 years, scientists and engineers have devoted more and more effort for solving problems related to the impact energy of solids. Until a couple of decades ago, the analysis of these problems turned almost exclusively to collisions of solids, of simple geometry and low impact energy, with limited plastic deformation, given mathematical complexity of the equations involved in these phenomena and the limited information available on the mechanical behavior of materials at high-speed deformation (Ref 5). Crack tip deformation and fracture parameter history in functionally graded glass-filled epoxy were evaluated for low velocity impact loading by Rousseau and Tippur (Ref 6). They showed when the crack growth occurs in a material with progressively increasing filler volume fraction, continuously increasing dynamic stress intensity factor is seen while a decreasing trend is observed when the gradient is of the opposite sense. Guo and Noda (Ref 7) studied the dynamic response of a functionally graded layered structure with a crack crossing the interface with in-plane impact loading condition. Xu et al. (Ref 8) investigated the plane strain problem of semi-infinite cracks in an infinite functionally graded orthotropic material with opening and in-plane shear impact loading modes. They have observed that the stress intensity factors are not all proportional to the square root of time as expected.

Functionally graded steels (FGSs) may be produced during welding of alloy steels. Charpy impact tests have been performed on functionally graded steels especially on the welded joints by several researchers. Hong et al. (Ref 9) performed the Charpy test with notch position varying within HAZ and reported that the absorbed energy is influenced by notch position with respect to various microstructures and it was reduced as notch position approach to the base material. Jang et al. (Ref 10) studied experimentally and numerically the effects of notch position on the failure behavior and energy absorption when the Charpy impact test was performed at -1 °C. Carbon steel plate with thickness of 25 mm was welded and specimens were fabricated from the welded plate. The Charpy impact tests were then performed on specimens having different notch positions varying within HAZ. A series of 3-D FE analysis which simulate the Charpy test were also carried out. Bezensek and Hancock (Ref 11) studied the toughness of laser welded joints of low alloy steel under mode I and mixed mode configuration along with Charpy impact tests. They observed that in Charpy tests, the crack deviated into the tougher parent plate giving potentially misleading indications of the behavior of defects in highly constrained joints.

Recently, FGSs have been produced by electroslag remelting (ESR) (Ref 12). Studies on transformation characteristics of FGSs produced from austenitic stainless steel and plain carbon steel have revealed that as chromium, nickel, and carbon atoms diffuse at remelting stage, alternating regions with different transformation characteristics are created. By selecting appropriate arrangement and thickness of original ferritic ($\dot{\alpha}$) and original austenitic ($\dot{\gamma}$) steels as electrodes, composites with graded ferrite, and austenite regions together

A. Nazari, Department of Technical and Engineering Sciences, Islamic Azad University (Saveh branch), Saveh, Iran; and **J. Aghazadeh Mohandesi**, Department of Mining and Metallurgical Engineering, Amirkabir University of Technology, 424, Hafez Avenue, Tehran, Iran. Contact e-mails: alinazari84@aut.ac.ir and agazad@yahoo.com.

with bainite or martensite layers may be made as follows (Ref 12);

$$(\dot{\alpha}\dot{\gamma})_{el} \xrightarrow{R} (\alpha\beta\gamma)_{com}$$

$$(\dot{\gamma}\dot{\alpha}\dot{\gamma})_{el} \xrightarrow{R} (\gamma M\gamma)_{com}$$

$$(\dot{\alpha}\dot{\gamma}\dot{\alpha})_{el} \xrightarrow{R} (\alpha\beta\gamma\beta\alpha)_{com}$$

$$(\dot{\alpha}\dot{\gamma}\dot{\alpha}\dot{\gamma})_{el} \xrightarrow{R} (\alpha\beta\gamma M\gamma)_{com}$$

$$(\dot{\gamma}\dot{\alpha}\dot{\alpha}\dot{\gamma})_{el} \xrightarrow{R} (\gamma\beta\alpha\beta\gamma)_{com}$$

where α and γ are graded ferrite and austenite regions in the final composite, respectively; β and M are bainite and martensite layers in the final composite, respectively; el is electrode; com is composite; and R is remelting.

The microhardness profile of composites is shown in Fig. 1 (Ref 13). The thickness of bainitic and martensitic layers were 0.6 and 1.5 mm, respectively. Also tensile strength of FGSs has been modeled based on the rule of mixtures (Ref 13). In this work, Charpy impact energy of αβγ and γMγ functionally graded steels with notch tip perpendicular to the graded layers (i.e., crack arrester configuration) has been studied.

2. Experimental Procedure

Similar to the previous works (Ref 12, 13), to make FGSs, a miniature ESR apparatus was utilized. The slag was a mixture of 20% CaO, 20% Al_2O_3, and 60% CaF_2. The original ferritic and austenitic steels which used as electrodes were commercial type AISI 1020 (with 0.2 wt.% C, 0.3 wt.% Si, 0.2 wt.% Mn, 0.05 wt.% S, and 0.05 wt.% P) and AISI 316 (with 0.07 wt.% C, 1 wt.% Si, 2 wt.% Mn, 0.045 wt.% S, 0.03 wt.% P, 18.15 wt.% Cr, and 9.11 wt.% Ni).

Several arrangements of ferritic and austenitic steel slices in the form of two-piece $\dot{\alpha}\dot{\gamma}$ electrode, three-piece $\dot{\gamma}\dot{\alpha}\dot{\gamma}$ and $\dot{\alpha}\dot{\gamma}\dot{\alpha}$ electrodes and four-piece $\dot{\gamma}\dot{\alpha}\dot{\alpha}\dot{\gamma}$ and $\dot{\alpha}\dot{\gamma}\dot{\alpha}\dot{\gamma}$ electrodes were spot welded. The height of each slice in the two-piece $\dot{\alpha}\dot{\gamma}$ electrode was 150 mm. In the three-piece $\dot{\gamma}\dot{\alpha}\dot{\gamma}$ and $\dot{\alpha}\dot{\gamma}\dot{\alpha}$ electrodes, the height of the middle slice was 25 mm and that of the neighboring slices was 137.5 mm. Finally in four-piece $\dot{\gamma}\dot{\alpha}\dot{\alpha}\dot{\gamma}$ and $\dot{\alpha}\dot{\gamma}\dot{\alpha}\dot{\gamma}$ electrodes, the height of the two middle slices was 25 mm and that of the neighboring slices was 125 mm.

Remelting was carried out under a constant power supply of 16 kVA. After remelting, composite ingots were hot-pressed at 980 °C down to the thickness of 30 mm and then were air-cooled.

The impact energy of FGSs in crack arrester configuration was evaluated by Charpy impact test at 18 °C using standard sized specimens (10 by 10 by 50 mm) according to the ASTM E23. The dimension of the specimens is shown in Fig. 2. From the produced αβγ and αβγMγ composite ingots, eight series of Charpy specimens were produced in which the bainite or martensite intermediate layers were situated at different positions with respect to the notch tip; in four series of specimens the notch was situated in alpha and in the other four in gamma region. For each series three specimens were tested and the average values were determined. From γMγ, αβγβα, and γβαβγ composite ingots, due to their symmetric configuration, only four series of Charpy impact specimens with different positions of bainite or martensite layers were produced. Charpy impact energy of as-received ferritic and austenitic steels which were annealed at 980 °C and then were air-cooled was measured. Also Charpy impact energy of single-phase bainite and martensite with composition and mechanical properties analogous to the bainite and martensite layers was measured. The production method of single-phase specimens with chemical composition and mechanical properties identical to the bainitic and martensitic layers in the studied composites was similar to the previous work (Ref 13). To do this, Charpy impact specimens of the same composition and mechanical properties to bainitic and martensitic layers in the studied composites were produced. Initially, the average chemical composition of bainite and martensite layers was obtained (Table 1). Afterward, bainitic and martensitic samples with composition in accordance to the average composition of single-phase bainitic and martensitic specimens were produced by means of a vacuum induction furnace. Similar to the primary composites, the hot-pressing process was carried out at 980 °C, followed by air cooling. Through trial and error (i.e., conforming the chemical composition and changing the cooling rate), the samples with the nearest hardness to single-phase bainitic and martensitic specimens were selected and Charpy impact test specimens from the bainitic and martensitic samples were made. Charpy impact test results of single-phase bainite and martensite layers produced from the sample are shown in Fig. 3.

3. Results and Discussion

Figure 4 illustrates Charpy impact energies of αβγ composites with notch tip at ferrite $\left(CV^{\alpha\beta\gamma}_{(\alpha_i)}\right)$ and austenite $\left(CV^{\alpha\beta\gamma}_{(\gamma_j)}\right)$ regions; where i and j equal to 0, 1, 2, 3 imply distances of the notch tip from the bainite layer (in millimeters) which was determined by metallographic studies. Charpy impact energy of the studied composites is between that of ferritic steel and austenitic steel. A number of studies have been conducted on the impact energy of layered materials, and it has been reported that Charpy impact energy of them is increased with respect to their constituent materials due to the delaminating of the layers when the interface strength between the layers is not high (Ref 14, 15). The stronger the interface, the more difficult the delamination, therefore it diminishes the impact properties (Ref 15). In the present study, since specimens were made by electroslag remelting, interface strength due to atomic diffusion is high, justifying the obtained results.

Figure 4 shows the variation of $CV^{\alpha\beta\gamma}_{(\gamma_j)}$ and $CV^{\alpha\beta\gamma}_{(\alpha_i)}$ with respect to the notch tip position. This could be discussed in terms of the consumed energy for plastic deformation under impact test. Generally the total energy consumed by a notched specimen till fracture under impact test may be expressed as;

$$E_t = E_e + E'_t + \sum_{i=1}^{N} (2\gamma)_i \qquad \text{(Eq 1)}$$

where E_e is the maximum energy absorbed by the elastic deflection (Ref 16), E'_t is the energy absorbed by the plastic

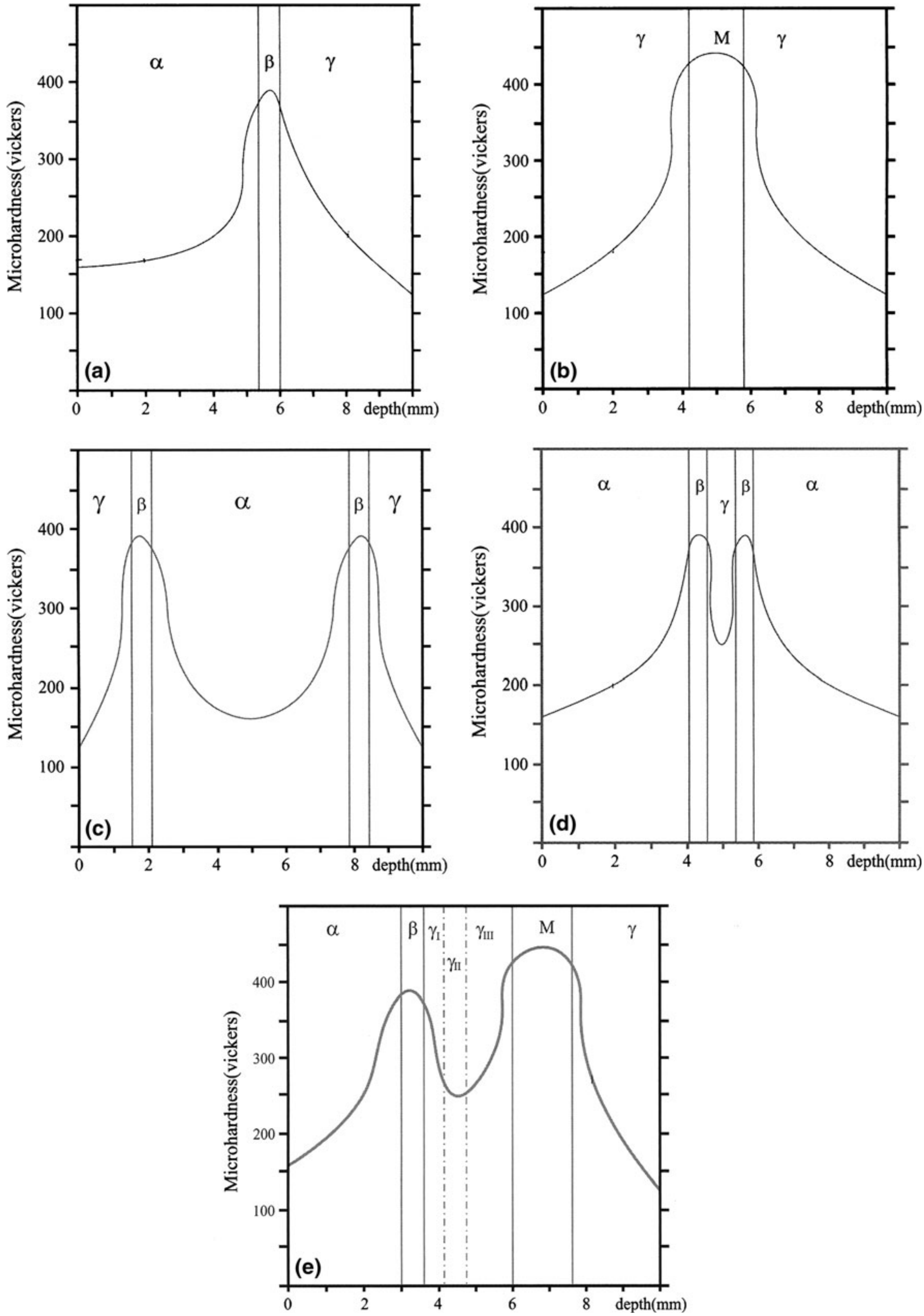

Fig. 1 Microhardness profile of (a) αβγ, (b) γMγ, (c) γβαβγ, (d) αβγβα, and (e) αβγMγ composite plates (Ref 13)

deformation ahead of the notch tip, and $\sum_{i=1}^{N}(2\gamma)_i$ is the total surface energy due to the formation of two new surfaces, and $2(\gamma)_i$ is the corresponding surface energy for crack growth in each graded layer.

It has been reported that the main impact value in a tough material is absorbed by the plastic zone ahead of the notch (Ref 17, 18). The volume of the plastically deformed material is very different; it amounts to several hundreds of mm^3 in the ductile range, and it is negligible in the brittle range. Virtually in a tough material more than 90% of the impact energy is consumed for the plastic deformation (Ref 19). This has also been confirmed for functionally graded steels by conducting instrumented Charpy impact studies (Ref 20). It has been pointed out that, with a good approximation, the plastic strain energy consumed for functionally graded steel under impact test may be assumed to be proportional to the corresponding area under stress-strain curve. An exponential relationship was found to correlate the area under stress-strain curve of each layer to its corresponding position in the graded region (Ref 21). Similarly an exponential relation may be assumed between Charpy impact energy of each layer and its corresponding position. Because the area under stress-strain curve of the consecutive layers in the alpha region gradually increases from the original ferrite to the bainite layer, one may expect that formation of the plastic zone ahead of the notch requires higher energy accordingly. While in the gamma region, because the area under stress-strain curve of the layers gradually decreases from original austenite to the bainite layer, one may expect that formation of the plastic zone at the notch tip requires lower energy. Hence, due to greater energy requirement for plastic deformation ahead of the notch tip in gamma region with respect to that of alpha region, as is illustrated in Fig. 4, $CV^{\alpha\beta\gamma}_{(\alpha_i)}$ is always less than $CV^{\alpha\beta\gamma}_{(\gamma_j)}$ except for the alpha region in the vicinity of bainite layer (i.e., $d_\beta \leq 0.74$ mm, which may be determined from Eq 2 and 3). The interesting point is that even when i and j are equal to zero (i.e., the notch tip is located at bainite layer interface) it is expected that $CV^{\alpha\beta\gamma}_{(\alpha_i)}$ and $CV^{\alpha\beta\gamma}_{(\gamma_j)}$ to be equal to the impact energy of single-phase bainite, however, the experimental results show otherwise. It seems that when the notch is situated at bainite-ferrite interface, plastic deformation zone at the notch tip needs more energy than that of single-phase bainite and by subsequent crack growth in the graded gamma phase further increase in plastic deformation energy occurs $\left(\text{i.e., } CV^{\alpha\beta\gamma}_{(\alpha_i)} > CV_\beta\right)$. On the other hand, when the notch is located at bainite-austenite interface where the plastic deformation energy is less than that of bainite in single-phase specimen, the plastic zone size decreases upon further crack growth in the graded ferrite region $\left(\text{i.e., } CV^{\alpha\beta\gamma}_{(\gamma_j)} < CV_\beta\right)$.

Also, the closer the notch tip to the bainite layer in alpha region, the higher the impact energy and inverse the closer the notch tip to the bainite layer in gamma region, the lesser the impact energy. Again this could be justified in terms of the energy absorbed for plastic deformation ahead of the notch tip.

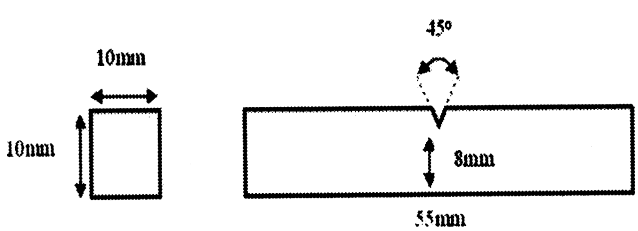

Fig. 2 Charpy impact test specimen dimensions

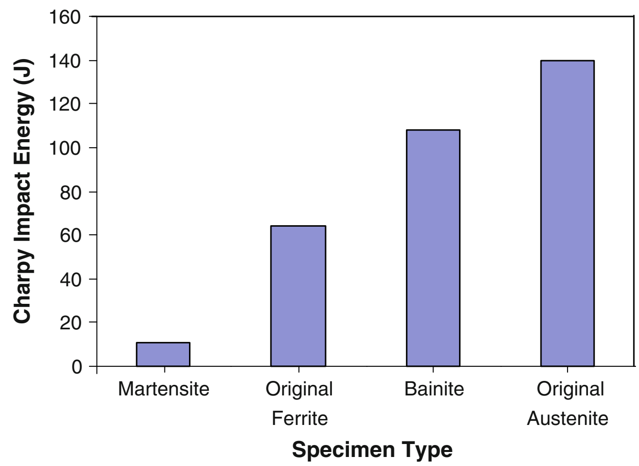

Fig. 3 Impact test results of the original ferrite, original austenite, single-phase bainite, and single-phase martensite specimens

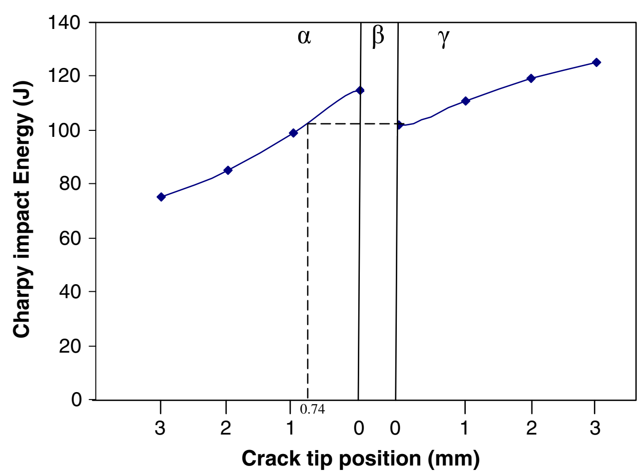

Fig. 4 Charpy impact energies of αβγ composites with different notch tip positions with respect to the bainite layer

Table 1 Chemical composition (wt.%) of bainitic and martensitic layers together with the single-phase bainite and martensite specimens produced from samples

Specimen studied	Pct Cr	Pct Ni	Pct C	Pct Si	Pct Mn	Pct S	Pct P
Single-phase bainite	14.5	7.2	0.12	0.8	1.8	0.03	0.04
Bainite specimen produced from the sample	14.7	7.15	0.13	0.85	1.9	0.032	0.045
Single-phase martensite	7.3	3.2	0.19	0.39	0.3	0.04	0.05
Martensite specimen produced from the sample	7.38	3.14	0.21	0.28	0.28	0.033	0.055

Figure 5 shows impact energies of different αβγ composites with notch tip in alpha region and together with the corresponding distances with respect to the bainite layer. Based on the given data, the best-fit equation to the experimental results was an exponential equation with coefficient of determination, $R^2 = 0.9981$ as follow;

$$CV_{(\alpha)}^{\alpha\beta\gamma} = 114.46\exp(-0.1435d_{\beta}) \quad \text{(Eq 2)}$$

where d_{β} is the distance of notch tip from the bainite layer.

Similarly, the best-fit equation for Charpy impact energies of αβγ composites with notch tip in gamma region is as below;

$$CV_{(\gamma)}^{\alpha\beta\gamma} = 102.88\exp(0.068d_{\beta}), \quad R^2 = 0.9866 \quad \text{(Eq 3)}$$

Charpy impact energies of γMγ composites $\left(CV_{(\gamma_i)}^{\gamma M\gamma}\right)$ are given in Fig. 6. Reduction of Charpy impact energy in the presence of martensite layer is very significant; the closer the notch tip to the martensite layer, the lesser the impact energy. Figure 7 shows two different positions of the notch tip with respect to the martensite layer in γMγ composite. Similar to αβγ composites, the difference between Charpy impact energies of γMγ composites may be explained in terms of plastic deformation energy. Note that due to greater thickness of martensite layer (i.e., 1.5 mm) and much smaller plastic zone ahead of notch with respect to the bainite layer, the difference between Charpy impact energy of γMγ composite with notch situated at martensite-austenite interface (i.e., $i = 0$) with that of single-phase martensite is not high. The relation between Charpy impact energy of γMγ composites with distance of notch tip with respect to the martensite layer could be represented as;

$$CV_{(\gamma)}^{\gamma M\gamma} = 13.166\exp(0.6127d_{M}), \quad R^2 = 0.9993 \quad \text{(Eq 4)}$$

where d_M is the distance of notch tip from the martensite layer.

Once more, for αβγβα, γβαβγ, and αβγMγ composites, the plastic zone size is able to justify the differences between Charpy impact energies of the same composites by situating the notch in different positions with respect to the bainite or martensite layers (Fig. 8-10). The interesting point is that when the notch is situated in alpha region of αβγMγ composite, Charpy impact energy of the composite is even higher than that of αβγ composite with similar distances of the notch with respect to the bainite layer whereas αβγMγ composite contains a brittle martensite layer. On the other hand, when the notch is situated in gamma region of αβγMγ composite, the impact

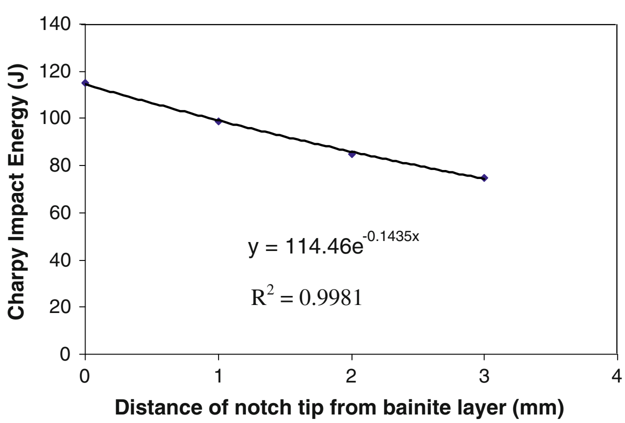

Fig. 5 Charpy impact energies of αβγ composites with notch tip in alpha region and the corresponding notch tip distance from bainite layer

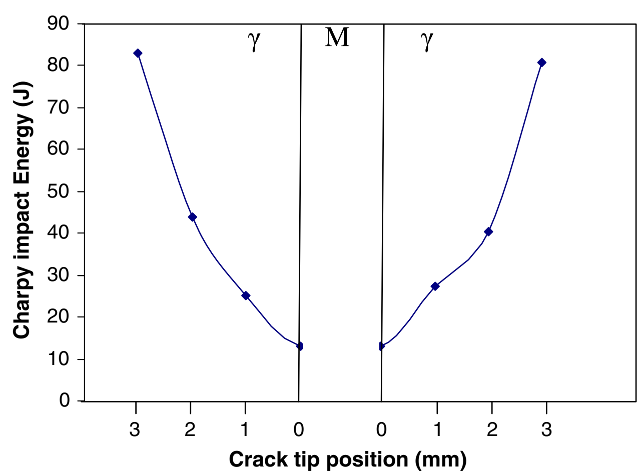

Fig. 6 Charpy impact energies of γMγ composites with different notch tip positions with respect to the martensite layer

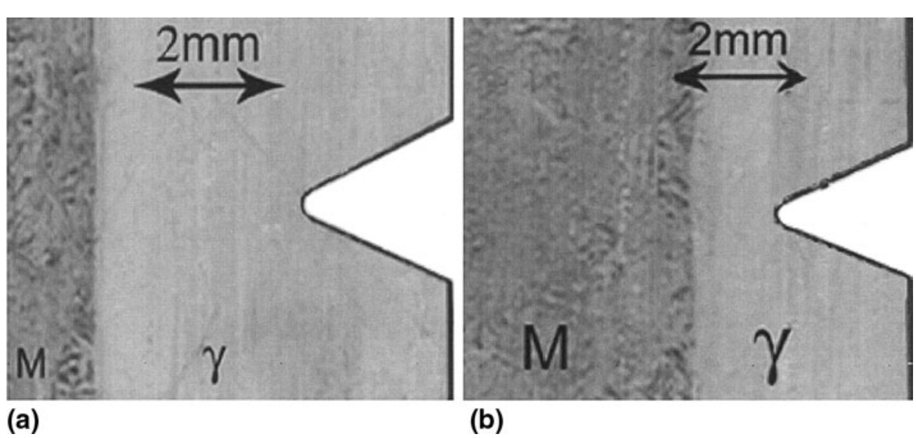

Fig. 7 Microstructure of γMγ composite illustrating positions of notch tip with respect to the martensite layer

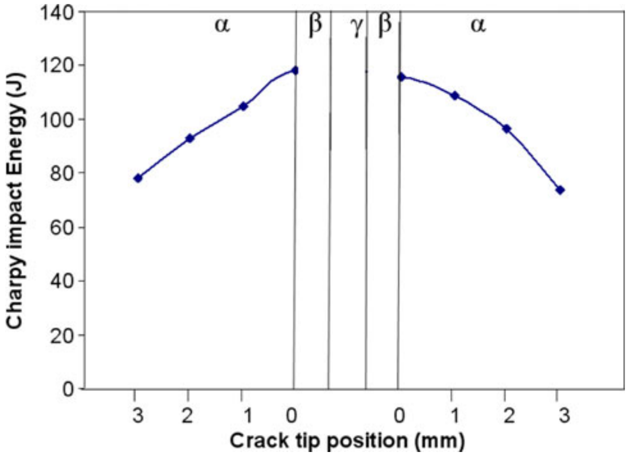

Fig. 8 Charpy impact energies of αβγβα composites with different notch tip positions with respect to the bainite layer

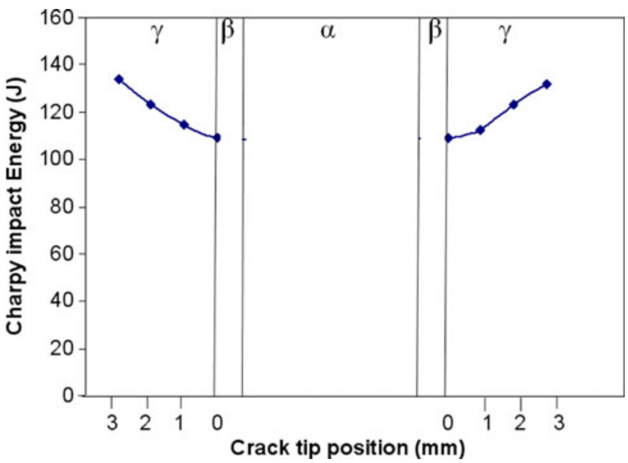

Fig. 9 Charpy impact energies of γβαβγ composites with different notch tip positions with respect to the bainite layer

energy is relatively low, particularly when the notch is situated too close to the martensite layer. Similarly, the relation between Charpy impact energies of αβγβα, γβαβγ, and αβγMγ composites with distance of notch tip with respect to the bainite or martensite layers could be empirically represented as;

$$\mathrm{CV}^{\alpha\beta\gamma\beta\alpha} = 119.46\exp(-0.1363 d_{\beta}), \quad R^2 = 0.9894 \qquad \text{(Eq 5)}$$

$$\mathrm{CV}^{\gamma\beta\alpha\beta\gamma} = 108.16\exp(0.0687 d_{\beta}), \quad R^2 = 0.9892 \qquad \text{(Eq 6)}$$

$$\mathrm{CV}^{\alpha\beta\gamma\mathrm{M}\gamma}_{(\alpha)} = 115.15\exp(-0.1302 d_{\beta}), \quad R^2 = 0.9925 \qquad \text{(Eq 7)}$$

$$\mathrm{CV}^{\alpha\beta\gamma\mathrm{M}\gamma}_{(\gamma)} = 14.593\exp(0.6347 d_{\mathrm{M}}), \quad R^2 = 0.9971. \qquad \text{(Eq 8)}$$

4. Conclusions

1. Although it would be possible to increase the impact resistance of AISI 1020 steel by producing functionally graded composites of the type αβγ, αβγβα, γβαβγ, γMγ, and αβγMγ, the high cohesive strength of α-β and β-γ interfaces causes no improvement in the impact properties respect to AISI 316 steel. Also, the formation of martensite layer in γMγ and αβγMγ composites decreases the impact resistance of 316 steel significantly.
2. The impact energy of the studied composites depends on the notch tip position in alpha or gamma regions in addition to its distance from bainite or martensite layers.
3. The impact energy of the studied composites may be explained in terms of plastic deformation zone ahead of the notch tip.

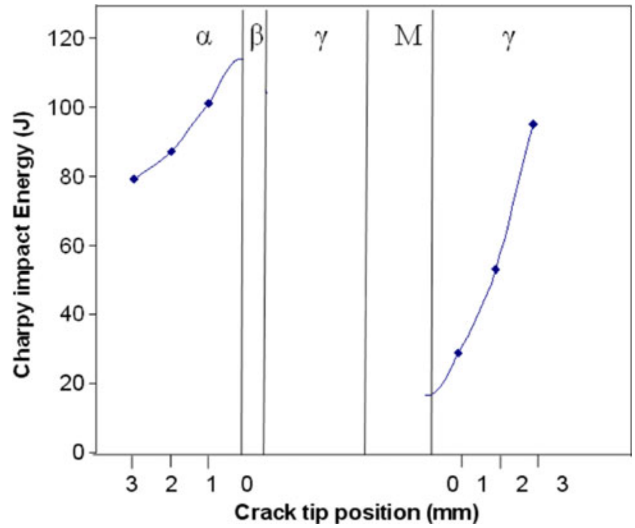

Fig. 10 Charpy impact energies of αβγMγ composites with different notch tip positions with respect to the bainite/martensite layer

References

1. I. Hofinger, H.A. Bahr, H. Balke, G. Kirchhoff, C. Häusler, and H.J. Weiß, Fracture Mechanical Modelling and Damage Characterization of Functionally Graded Thermal Barrier Coatings by Means of Laser Irradiation, *Mater. Sci. Forum*, 1999, **308-311**, p 450–456
2. Z.H. Jin, G.H. Paulino, and R.H. Dodds, Finite Element Investigation of Quasi-static Crack Growth in Functionally Graded Materials Using a Novel Cohesive Zone Fracture Model, *J. Appl. Mech.*, 2002, **69**, p 370–379
3. S. Pal, M.G. Kulkarni, and D.V. Kubair, Mode-3 Spontaneous Crack Propagation in Symmetric Functionally Graded Materials, *Int. J. Sol. Struc.*, 2007, **44**, p 242–254
4. C.E. Rousseau and H.V. Tippur, Compositionally Graded Materials with Cracks Normal to the Elastic Gradient, *Acta Mater.*, 2000, **48**(16), p 4021–4033
5. W. Goldsmith, *Impact: The Theory and Physical Behaviour of Colliding Solids*, Edward Arnold Publishers, London, 1960
6. C.E. Rouseau and H.V. Tippur, Dynamic Fracture of Compositionally Graded Materials with Cracks Along the Elastic Gradient: Experiments and Analysis, *Mech. Mater.*, 2001, **33**, p 403–421
7. L.C. Guo and N. Noda, Dynamic Investigation of a Functionally Graded Layered Structure with a Crack Crossing the Interface, *Int. J. Sol. Struc.*, 2008, **45**, p 336–357
8. H. Xu, X. Yao, X. Feng, and Y.Y. Hisen, Dynamic Stress Intensity Factors of a Semi-infinite Crack in an Orthotropic Functionally Graded Material, *Mech. Mater.*, 2008, **40**, p 37–47
9. J.K. Hong, Y.H. Son, J.H. Park, B.H. Lee, S.C. Yoon, and C.G. Kang, *Proceeding of 15th International Conference on Nuclear Engineering 2007*, Japan

10. Y.C. Jang, J.K. Hong, J.H. Park, D.W. Kim, and Y. Lee, Effects of Notch Position of the Charpy Impact Specimen on the Failure Behavior in Heat Affected Zone, *J. Mater. Proc. Tech.*, 2008, **201**, p 419–424
11. B. Bezensek and J.W. Hancock, The Toughness of Laser Welded Joints in the Ductile-Brittle Transition, *Eng. Fract. Mech.*, 2007, **74**, p 2395–2419
12. J. Aghazadeh Mohandesi and M.H. Shahosseinie, Transformation Characteristics of Functionally Graded Steels Produced by Electrosag Remelting, *Metall. Trans. A*, 2005, **36A**, p 3471–3476
13. J. Aghazadeh Mohandesi, M.H. Shahosseinie, and R. Parastar Namin, Tensile Behavior of Functionally Functionally Graded Steels Produced by Electroslag Remelting, *Metall. Trans. A*, 2006, **37A**, p 2125–2132
14. B.T. Marouf, R. Bagheri, and R. Mahmudi, Role of Interfacial Fracture Energy and Laminate Architecture on Impact Performance of Aluminum Laminates, *Composites A*, 2008, **39**(11), p 1685–1693
15. F. Carreno, J. Chao, M. Pozuelo, and O.A. Ruano, Microstructure and Fracture Properties of an Ultrahigh Carbon Steel-Mild Steel Laminated Composite, *Scripta Mater.*, 2003, **48**, p 1135–1140
16. J.P. Tronskar, M.A. Mannan, and M.O. Lai, Measurement of Fracture Initiation Toughness and Crack Resistance in Instrumented Charpy Impact Testing, *Eng. Fract. Mech.*, 2002, **69**, p 238–321
17. F. Vodopivec, B. Arzenšek, D. Kmetič, and J. Vojvodič-Tuma, On the Charpy Fracturing Process, *MTAC9*, 2003, **37**(6), p 317–326
18. F. Vodopivec, B. Arzenšek, J. Vojvodič-Tuma, and R. Celin, The Charpy Fracturing Process in Ductile Range, *METBAK*, 2008, **47**(3), p 173–179
19. D.W. Kum, T. Oyama, O.A. Ruano, and O.D. Sherby, Development of Ferrous Laminated Composites with Unique Microstructures by Control of Carbon Diffusion, *Metall. Trans. A*, 1986, **17**, p 1517–1521
20. A. Nazari and J. Aghazadeh Mohandesi, Modeling Impact Energy of Functionally Graded Steels in Crack Arrester Configuration, To be published
21. A. Nazari and J. Aghazadeh Mohandesi, Modeling Impact Energy of Functionally Graded Steels in Crack Divider Configuration, *Mater. Sci. Technol.*, To be published